

CONFORMAL MAPPING POTENTIAL FLOW AROUND A WINGSECTION USED AS A TEST CASE FOR THE INVISCID PART OF RANS SOLVERS

Björn Regnström*

*Flowtech International AB,
 Chalmers Tvärgata 10
 PO Box 24001
 SE 40022 Göteborg, Sweden
 e-mail: regnstrom@flowtech.se

Key words: Fluid Dynamics, Verification , Analytic Solution, Potential Flow, Conformal Mapping, Wing Section

Abstract. *The Theodorsen-Garrick conformal mapping is used to make a grid around a wing section and to compute the potential flow around it. The potential flow is a solution to the incompressible Euler equations and can be used to verify the inviscid part of RANS codes.*

1 INTRODUCTION

The ideal test for a CFD code is of course an analytic solution. Analytic solutions to the Navier Stokes or RANS equations are however restricted to specific geometries. Using manufactured solutions gets around this limitation but the test functions are not physical so even though conclusions about the order of accuracy of the method and the relative size of the errors can be drawn there is no direct connection to how the errors affects for instance the integrated forces.

In the present work a potential flow solution from a conformal mapping of a wing section is proposed for verification of the inviscid part of RANS codes.

2 CONFORMAL MAPPING

To transform the region on and outside of a wing section the method of Theodorsen and Garrick is used^{1,2}. The transformation is done in three steps. First a Karman-Treffitz transform is used to remove the trailing edge corner.

$$\left(\frac{\zeta' - \beta z_0}{\zeta' - \beta z_1} \right) = \left(\frac{z - \beta z_0}{z - \beta z_1} \right)^{1/\beta} \quad (1)$$

where $\beta = 1/(2 - \tau/\pi)$. The transform is singular in the points z_0 and z_1 and corners with an included angle τ in these points are transformed to have a continuous derivative in the ζ' -plane. For normal wing sections with a sharp trailing edge and a smooth leading edge, z_0 is set to the trailing edge location while z_1 is located inside of the wing section. The actual location of z_1 is arbitrary, but the image of the wing section is close to a circle in the ζ' -plane if it is placed halfways between the point of maximum curvature and its centre of curvature.

The next step is a translation

$$\zeta = \zeta' - \zeta'_c \quad (2)$$

where ζ'_c is the coordinates of the centroid of the curve in the ζ' -plane. Centering the curve on the origin together making with it into a near circle in the previous step improves the convergence of the last step which is the Theodorsen-Garrick transform

$$\zeta = \xi e^{\sum_{j=0}^n (a_j + ib_j) \xi^{-j}} \quad (3)$$

2.1 Computation of mapping constants

The wing section is given as offset points p_0, \dots, p_m starting at the trailing edge, going forward on the upper side, round the leading edge and back on the lower side back to the trailing edge. In the following the trailing edge is assumed to be in the point $(1,0)$ and the leading edge in $(0,0)$ so $z_0 = 1 + i0$.

To determine z_1 the point of maximum curvature is approximated by the offset point closest to the leading edge $p_L : \Re p_L = \min \Re p_j$ and the centre of curvature c_{LE} is found by fitting a circle to the three points p_{L-1}, p_L, p_{L+1} . Finally, $z_1 = \frac{1}{2}(p_L + c_{LE})$.

The translation constant ζ'_c is calculated as

$$\zeta'_c = \frac{\oint \zeta' d\zeta'}{\oint d\zeta'} \approx \frac{\sum_{j=0}^{m-1} \frac{\zeta'_{j+1} + \zeta'_j}{2} |\zeta'_{j+1} - \zeta'_j|}{\sum_{j=0}^{m-1} |\zeta'_{j+1} - \zeta'_j|} \quad (4)$$

where $\zeta'_0, \dots, \zeta'_m$ are the offset points transformed to the ζ -plane by the Karman-Trafftz transform. The transform in this direction involves fractional powers of $z - z_0$ and $z - z_1$ so a tracking procedure that keeps the argument continuous by switching Riemann sheet when needed is used.

The hardest work is to determine the constants $a_j + ib_j$ of the Theodorsen-Garrick transform that maps the near circle in the ζ -plane to a unit circle in the xi -plane. First express ζ and ξ in polar coordinates

$$\begin{aligned} \zeta &= re^{i\theta} \\ \xi &= e^{i\phi} \end{aligned} \quad (5)$$

Substitute (5) into (3) and take the logarithm of both sides. The real and imaginary parts of the equation are

$$\ln r = a_0 + \sum_{j=1}^n (a_j \cos j\phi + b_j \sin j\phi) \quad (6)$$

$$\theta = \phi + b_0 + \sum_{j=1}^n (b_j \cos j\phi - a_j \sin j\phi) \quad (7)$$

To place the trailing edge at $\phi = 0$ let

$$\theta_T E = b_0 + \sum_{j=1}^n b_j \quad (8)$$

where $\theta_T E = \arg \zeta_0$. Evaluate the equation for the angle (7) for $2n$ uniformly spaced angles

$$\phi_k = 2\pi \frac{k}{2n} \quad k = 0, \dots, 2n-1 \quad (9)$$

which gives $2n$ equations. With b_0 determined from (8) there are $2n+1$ parameters a_j, b_j to determine. Since there is one equation less than parameters, one parameter can be chosen freely. With $b_n = 0$ the equations for the angles are

$$\theta_k - \phi_k = b_0 + \sum_{j=1}^{n-1} (b_j \cos j\phi_k - a_j \sin j\phi_k) \quad (10)$$

By re-writing the parameters as

$$\begin{aligned} y_0 &= b_0 \\ y_j &= \text{frac12}(b_j + ia_j) \quad j = 1, \dots, n-1 \\ y_n &= 0 \\ y_{2n-j} &= \overline{y_j} \quad j = 1, \dots, n-1 \end{aligned} \quad (11)$$

the right hand side of (10) can be expressed as a discrete Fourier transform that can be efficiently evaluated with FFT.

$$\theta_k - \phi_k = \sum_{j=0}^{2n-1} y_j e^{2\pi i \frac{jk}{2n}} \quad (12)$$

Having thus determined the angles θ_k an updated set of parameters a_j, b_j is computed with the inverse transform

$$y_j = \frac{1}{2n} \sum_{k=0}^{2n-1} lnr(\theta_k) e^{-2\pi i \frac{jk}{2n}} \quad (13)$$

where

$$\begin{aligned} a_0 &= y_0 \\ a_n &= y_n \\ a_j &= 2\Re y_j \quad j = 1, \dots, n-1 \\ b_j &= -2\Im y_j \quad j = 1, \dots, n-1 \end{aligned} \quad (14)$$

y_0 and y_n are real and $y_{2n-j} = \overline{y_j}$, $j = 1, \dots, n-1$ since y_j are the Fourier coefficients of a real sequence. The values $lnr(\theta_k)$ are obtained from a periodic cubic spline fit³ to the original points $\ln |\zeta_j|$.

The equations (12) and (13) are used iteratively to compute the parameters. The iterations are started by setting $a_j = b_j = 0$ except for $b_0 = \theta_T E$. Then (12) is applied to compute the angles and finally (13) gives an updated set of parameters. The iterations continue until the parameters have converged to sufficiently high accuracy. Sufficient conditions for the convergence of this scheme are⁴

$$\begin{aligned} (r_{max}/r_{min})^{1/2} - 1 &< \epsilon & (15) \\ \left| \left(\frac{\partial \ln r}{\partial \theta} \right)_{max} \right| &< \epsilon \\ \epsilon &= 0.2954976 \end{aligned}$$

There are several approximations involved in the determination of the mapping parameters, but they do not introduce any errors when the transform is used for verification since the grid and the potential flow solution are calculated with exactly the same parameters. Compare this to the situation if a panel method was used to generate a reference solution. Then there could be differences in geometry due to different grid generators being used, and there would also be errors due to the finite resolution of the panels.

2.2 Grid generation

Nodes for a structured grid is generated by transforming a cartesian grid in the polar coordinates (r, ϕ) , $r \in [1, r_{max}]$, $\phi \in [0, 2\pi]$ of the xi -plane to the z -plane. If the section is symmetrical a grid around one half can be generated by $\phi \in [0, \pi]$. The half grid may be used to test the implementation of the symmetry boundary condition. Another variation is add a constant to ϕ to test the influence of the position of the periodic boundary.

The transform concentrates points in the leading and trailing edge regions, so there is no need to stretch the grid in the angular direction. In the radial direction it may be advantageous to stretch towards $r=1$, see the figure below.

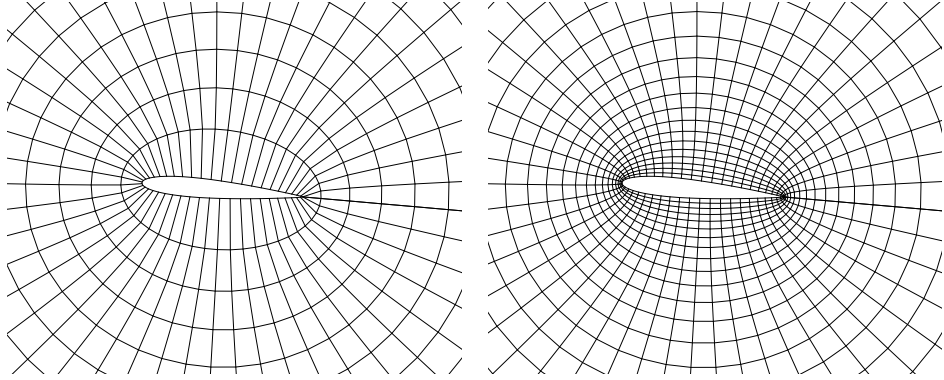


Figure 1: Unstretched grid (left) and radially stretched grid (right).

3 POTENTIAL FLOW SOLUTION

If $\xi(z)$ is a conformal mapping, then the gradient and Laplacian of a scalar field ϕ transform as

$$\nabla\phi(z) = \frac{\nabla\phi(\xi)dz/d\xi}{|dz/d\xi|^2} \quad (16)$$

$$\nabla^2\phi(z) = \frac{\nabla^2\phi(\xi)}{|dz/d\xi|^2} \quad (17)$$

For exterior flow around a body in uniform flow the boundary conditions on the body and far away are respectively

$$\frac{\partial\phi}{\partial n} = 0 \quad (18)$$

$$\nabla\phi \rightarrow \vec{U}_\infty \quad (19)$$

The first condition is unaffected by the transformation and the second is fulfilled if $|dz/d\xi| \rightarrow 1$ as $|xi| \rightarrow \infty$.

The potential flow solution around a unit circle in the ξ -plane that fulfills the Kutta condition of tangential flow (or stagnated for finite trailing edge angle) is

$$\phi = \phi_\infty + \phi_\mu + \phi_\gamma \quad (20)$$

$$\phi_\infty = rU_\infty \cos(\xi - \alpha) \quad (21)$$

$$\phi_\mu = -\frac{\mu \cos(\xi - \alpha)}{2\pi r} \quad (22)$$

$$\phi_\gamma = \frac{\gamma\xi}{2\pi} \quad (23)$$

where α is the angle of attack. The boundary conditions gives the source strengths

$$\mu = -2\pi U_\infty \quad (24)$$

$$\gamma = 4\pi U_\infty \sin(\alpha - \xi_T E) \quad (25)$$

The transformation derivative is

$$\frac{\partial z}{\partial \xi} = \frac{(1+D)EQ^{1/\beta-1}(z_1 - z_0)^2}{(Q^{1/\beta} - 1)^2(\beta - E\xi - \zeta'_c)^2} \quad (26)$$

$$D = \sum_{j=0}^n (a_j + ib_j)j\xi^{-j} \quad (27)$$

$$E = e^{\sum_{j=0}^n (a_j + ib_j)\xi^{-j}} \quad (28)$$

$$Q = \frac{\zeta'_c + E\xi - \beta z_1}{\zeta'_c + E\xi - \beta z_0} \quad (29)$$

The mapping derivative does not fulfil condition that $|dz/d\xi| \rightarrow 1$ as $|xi| \rightarrow \infty$ since the near circle has to be scaled to become a unit circle in the ξ -plane. The scale factor is e^{-a_0} so the velocity field in the z -plane is

$$u = \nabla \phi(\xi) dz/d\xi = \frac{\nabla \phi(\xi) dz/d\xi}{|dz/d\xi|^2} e^{-a_0} \quad (30)$$

The static pressure is given by Bernoulli's equation. With the reference pressure $p_\infty = 0$

$$p = \frac{\rho}{2}(U_\infty^2 - u^2) \quad (31)$$

4 CONCLUSIONS

- The Theodorsen-Garrick transform has been implemented and integrated in the SHIPFLOW code. Grids and velocity and pressure fields can be computed.
- CPU time to compute mapping parameters, grids and field are negligible.
- The reference solution is exact in the sense that it is an analytical solution for the mapped geometry.
- Things that can be tested:
 - Discretisation of incompressible Euler equations.
 - Solution of incompressible Euler equations.
 - Implementation of symmetry boundary condition.

- Integration of pressure force.
- By extruding the grid in the third dimension and transpose the indices in the structured grid arrays a substantial part of the 3D implementation can also be tested.
- For testing of more complicated topologies, multi-element wing section mappings that are a generalisation of the above are available^{1,2}.

REFERENCES

- [1] D.C. Ives. A modern look t conformal mapping including multiply connected regions. *AIAA Journal*, **14**(8), 1006–1011, (1976)
- [2] N.D.Halsey. Potential flow analysis of multielement airfoils using conformal mapping. *AIAA Journal*, **17**(12), 1281–1288, (1979)
- [3] Mortensen. Geometric Modeling. John Wiley & Sons.
- [4] S.E. Warschawski. On Theodorsen's method of conformal mapping of nearly circular regions. *Quarterly of Applied Mathematics*, **3**, 12–28, (1945)